Pharmaceutical Sciences. 2026;32(1):102-109
doi:10.34172/PS.026.43381
https://ps.tbzmed.ac.ir/

Original Article

The Modulatory Effect of Liraglutide on the Expression of GPX4, HO-1 and SLC7A11 Signaling Pathway in Obese Rats

Mahmood Jameel Saeed*, Inam Sameh Arif

Department of Pharmacology and Toxicology, College of Pharmacy, Mustansiriyah University, Baghdad, Iraq

ARTICLE INFO

Article History:
Received: September 30, 2025
Revised: November 11, 2025
Accepted: November 22, 2025
ePublished: January 5, 2026

Keywords:
Obesity, Ferroptosis, Liraglutide, GPX4, HO-1, SLC7A11

Abstract

Background: Obesity, a multifaceted metabolic condition, is associated with oxidative stress and disrupted redox homeostasis, leading to ferroptosis and metabolic dysfunction. Liraglutide, a well-known glucagon-like peptide-1 (GLP-1) receptor agonist, is used in the treatment of obesity. This study aimed to examine the modulatory effects of liraglutide on oxidative stress and ferroptosis-related indicators in obese rats induced by high-fat diet (HFD).

Methods: Thirty-five male Wistar rats were randomly divided into five groups: a control group, an HFD-induced obesity group, and three liraglutide treatment groups (100, 200, and 400 µg/kg/day). Following a 4-week induction of HFD, liraglutide was administered subcutaneously for 28 days. Redox and ferroptosis changes were assessed by measuring serum iron, TfR-1, malondialdehyde (MDA), and superoxide dismutase (SOD), along with gene expression of SLC7A11 and the immunohistochemical expression of heme oxygenase-1 (HO-1) and glutathione peroxidase 4 (GPX4) in hepatic tissues.

Results: HFD-induced obesity significantly reduced the expression of antioxidant and ferroptosis-regulatory markers. Liraglutide treatment, particularly at high doses, significantly reversed these effects by upregulating SLC7A11 gene expression and enhancing HO-1, and GPX4 protein expression in a dose-dependent manner.

Conclusion: These findings suggest that liraglutide restores antioxidant capacity and inhibits ferroptosis through activation of the SLC7A11/HO-1/GPX4 axis. Beyond its metabolic benefits, liraglutide exerted cytoprotective effects, highlighting its potential therapeutic role in obesity-associated oxidative stress and ferroptosis injury.

Introduction

Obesity is a significant, chronic, intricate, and relapsing condition characterized by alterations in adipose tissue mass, distribution, or function, and has been associated with considerable morbidity and increased mortality rates.[1] Genetic, environmental, physiological, behavioral, and sociocultural factors all interact to cause obesity.[2] In general, a variety of factors influencing energy intake and expenditure contribute to development of obesity with food consumption or feeding habits being the primary determinants of energy intake.

Ferroptosis is a regulated form of cell death defined by iron (Fe^{2+})-dependent lipid peroxidation induced by reactive oxygen species (ROS).[3] The presence of cellular labile iron can induce ferroptosis.[4] Fe^{2+}acts as a catalyst in the transformation of HO_2 into $OH^{\bullet}$ radicals via the Fenton reaction, which then react with polyunsaturated fatty acids. Furthermore, Fe^{2+}functions as a cofactor for lipoxygenases, promoting the synthesis of lipid hydroperoxides.[5]

Abnormal differentiation and accumulation of adipose tissue frequently result in central obesity. An environment with high iron levels may lead to abnormal adipose tissue differentiation, potentially causing metabolic dysfunctions.[6] Reduction of iron levels through the knockdown of mitoferrin 1 and 2 (Mfrn1/2) in 3T3-L1 preadipocytes,[7] as well as the ablation of TfR-1 and the application of DFO, has been shown to result in atypical adipocyte differentiation,[8] suggesting that iron availability is crucial for the growth and differentiation of adipocytes. Animal studies further suggest that lowering iron concentrations in white adipose tissue may reduce intestinal lipid absorption and protect mice against metabolic disorders linked to a high-fat diet (HFD).[9]

Nrf2 (Nuclear factor erythroid 2-related factor 2) is a transcription factor that, under normal circumstances, translocates into the nucleus, where it interacts with antioxidant response elements (AREs) in the promoter regions of target genes, thereby stimulating their transcription.[10] The Nrf2 pathway plays an essential role in inhibiting lipid peroxidation-induced ferroptosis by upregulating genes such as SLC7A11, heme oxygenase-1 (HO-1) and glutathione peroxidase 4 (GPX4). The SLC7A11 gene (solute carrier family 7 member 11)

***Corresponding Author:** Mahmood Jameel Saeed, Email: Mahmood.jameel@uomustansiriyah.edu.iq

encodes a subunit of the cystine/glutamate antiporter, which is crucial for glutathione production, whereas GPX4 utilizes glutathione to neutralize lipid peroxides, thereby protecting cellular components from peroxidation and damage.[11] HO-1 catalyzes the breakdown of heme, a pro-oxidant compound, into biliverdin, free iron, and carbon monoxide (CO). Biliverdin is subsequently converted into bilirubin by biliverdin reductase, which has significant antioxidant properties. Thus, the degradation of heme not only lowers oxidative stress but also generates compounds with protective functions.[12]

Liraglutide is a synthetic glucagon-like peptide-1 (GLP-1) receptor agonist,[13] used primarily for the treatment of type 2 diabetes and obesity.[14,15] It is a long-acting analog of human GLP-1, structurally modified to increase its half-life, thereby enabling once-daily administration. In contrast to earlier research that explored liraglutide's anti-ferroptotic properties in hepatic ischemia-reperfusion injury[16] or diabetic cardiomyopathy[17] through GSK3β/Nrf2- or AKT/mTOR/NRF2-dependent mechanisms, the present study specifically examines the integrated regulation of the SLC7A11, HO-1, and GPX4 signaling pathway in obesity induced by an HDF.

Additionally, it seeks to assess the protective, antiapoptotic effect of GLP-1 agonists in male rats with diet-induced obesity.

Methods

Materials

Drugs and chemicals

Liraglutide (Rhawn, China) was used as the primary drug. Other reagents included eosin (Thomas Baker, India), ethanol (99%) and formalin (10%) (Scharlau, Spain), hematoxylin (Gourilabs, France), paraffin wax (Scharlau, Spain), xylene (Scharlau, Spain), ketamine 10% (Kepro Holland, India), xylazine 2% (Scharlau, Spain), normal saline (Pioneer, Iraq), and Trizol reagent (TransGen Biotech, China). GPX4 and HO-1 polyclonal antibodies for immunohistochemistry were obtained from Fine Test (China). ELISA kits for transferrin receptor-1 (TfR-1), superoxide dismutase (SOD), and serum iron were purchased from Cloud-clone Corp. (USA), while the malondialdehyde (MDA) ELISA kit was obtained from MyBioSource (USA).

Instruments

Instruments used included a spectrophotometer (Apel, Japan), centrifuge (Hettich Universal, Germany), micropipettes (Dragon Lab, China), analytical balance (Shimadzu, Japan), and water bath/heating block (Thermo Scientific, USA).

Animals

Thirty-five male Wistar albino rats, weighing 150–200 g, were used. The animals were handled in accordance with the laboratory animal ethics code and housed in appropriate cages within a well-ventilated facility at the College of Pharmacy. Conditions were maintained at 24 °C and 50% humidity, with unrestricted access to food and water. The rats were acclimated for one week prior to the experiment.

Experimental design

Group 1(G1, control) received distilled water. Group 2 (G2, induction) consisted of rats subjected to obesity using an HFD. Groups 3–5 were treatment groups that received liraglutide at doses of 100, 200, and 400 μg/kg/day, respectively, dissolved in distilled water and delivered subcutaneously for 28 days following 28 days of HFD induction.[18]

Experimental periods and ethical approval

The experiment started was conducted between 18 October and 25 December 2024. The period included 10 days of acclimatization, 4 weeks of HFD induction, and by 4 weeks of liraglutide administration, followed by with the euthanasia and sample collection. Ethical approval was obtained from the College of Pharmacy, Mustansiriyah University, Baghdad, Iraq (file no:53, dated 18/10/2024).

Sample collection

At the end of the experiment, rats were euthanized by intramuscular administration of 50 mg/kg ketamine and 5 mg/kg xylazine.[19] Blood samples were collected from the heart using a 5 mL syringe.[20] Samples were placed in gel tubes at ambient temperature for 20 minutes and subsequently centrifuged at 2500 rpm for 15 minutes for serum separation. Serum was collected in an Eppendorf tube and stored at -20 °C for oxidative stress and transferrin receptor-1 analysis.

Liver tissues were excised, cleaned of adherent tissues, and rinsed with distilled water. portions were preserved in 10% formalin for the purpose of immunohistochemical analysis.

A 50–100 mg liver sample was stored in 1 mL of Trizol in Eppendorf tubes and refrigerated for gene expression analysis via real-time PCR.

Colorimetric determination of serum iron

In an acidic solution with a reductant, ferric ions were released from transferrin and reduced to ferrous ions (Fe^{+2}). The latter subsequently is bound to bipyridine, forming pink complexes. iron concentration was determined by measuring optical density (OD) at 520 nm.[21]

Enzyme-linked immunosorbent assay (ELISA)

TfR-1, SOD, and MDA levels in tissue homogenate were measured using sandwich ELISA technique according to the manufacturer's protocol. Microplates pre-coated with monoclonal antibodies specific to each marker were incubated with samples and standards. Bound antigens were detected with biotinylated polyclonal antibodies, followed by avidin-conjugated HRP. After washing,

substrate solution (3,3,5,5' tetramethyl-benzidine; TMB) was added, generating a blue color proportional to antigen concentration. Reactions were terminated with H_2SO_4, producing a yellow color, which was quantified at 450 ± 2 nm using a spectrophotometer.

Immunohistochemical assay

Following the preparation of paraffin-embedded sample blocks and the cutting of a 4 µm sections onto charged slides, the following procedures were performed. Slides were incubated in a hot air oven at 65 °C for 30 minutes, followed by deparaffinization with xylene. Slides were then hydrated through a series of graded alcohols (100%, 90%, 80%, 70% distilled water) for 5 minutes each, ending with distilled water.

Nonspecific binding sites were blocked using a tissue block. Sections were incubated with 3% H_2O_2 (peroxidase block) for 5–10 minutes at ambient temperature, followed by washing with phosphate-buffered saline (PBS). A standard goat blocking buffer was applied for 30 minutes. Antigen retrieval was performed in Tris-EDTA buffer (pH 9) for 40 minutes, then cooled to room temperature and transferred to wash buffer at pH 7.4.

The primary antibodies were applied at the appropriate dilutions (GPX4, 1:50; HO-1, 1:100) and incubated overnight at 4 °C. Slides were then rewarmed and washed 2–3 times with PBS and dried, then incubated with secondary antibody for 20 minutes, followed by a 10-minute PBS wash. Diaminobenzidine (DAB) working solution was applied for 5 minutes to visualize positive staining as a tan/brown color, followed by a 5-minute buffer wash. Subsequently, sections were counterstained with hematoxylin for 2 minutes, followed by washing with buffer, then rinsed with tap water and dehydrated in graded alcohol solutions (70%, 80%, 95%, and 99.9%) for 1 minute each. Finally, slides were cleared in xylene and mounted with a cover slip.

Immunohistochemical expression of GPX4 and HO-1 was assessed semi-quantitative by combining staining intensity and the percentage of positive cells. The staining intensity was scored as 0 for no stain, 1 for weak, 2 for moderate, and 3 for strong. The percentage of immunoreactive cells was graded as follows: grade 0 = 0% (no stained cells), 1 = 1–25% stained cells, 2 = 25–50% stained cells, 3 = 50–75% stained cells, and 4 = 75–100% stained cells.

Gene expression assay

Approximately 50–100 g of liver tissue was placed into Eppendorf tubes containing 1 mL of Trizol and stored in a deep freeze for gene expression analysis. Total RNA was isolated using the RNA extraction kit (Transcript), followed by the synthesis of cDNA from total RNA using the cDNA synthesis supermix kit (Transcript).

Quantitative real-time PCR (qRT-PCR) was performed to quantify the SLC7A11 gene expression according to the manufacturer's protocol. The primer sequences of SLC7A11 were as follows: forward primer 5′-CCTCTGTTCATCCCAGCATT-3′ and reverse primer 5′-GGACCCCAGTCAAGGTGATA -3′. The reaction mixture was subjected to thermal cycling in a qRT-PCR apparatus.

Statistical analysis

All statistical analyses were conducted using IBM SPSS Statistics for Windows, Version 26.0 (IBM Corp., Armonk, NY, USA) and GraphPad Prism, Version 9.0 (GraphPad Software, San Diego, CA, USA). Microsoft Excel 2016 and Python (Matplotlib library, Version 3.8) were used for figure generation and advanced data visualization. One-way analysis of variance (ANOVA) was applied to assess differences among groups, contingent on meeting assumption of normality and homogeneity of variance. When significant differences were identified ($P < 0.05$), Tukey's post hoc test was used for pairwise comparisons. Data are presented as mean ± standard deviation (SD). All statistical tests were conducted as two-tailed, with a P value < 0.05 considered statistically significant.

Results

Iron status

Figure 1 illustrates the effects of liraglutide on iron homeostasis and ferroptosis-related parameters in HFD-induced obese rats. The HFD group (G2) demonstrated the highest mean serum iron concentration (246.71 ± 25.08 µg/dL) along with the highest level of transferrin receptor 1 (34.41 ± 4.96 ng/mL). Both values were significantly elevated compared with all other groups ($P < 0.05$ for all pairwise comparisons with G2), indicating a marked disruption of iron homeostasis following HFD induction.

Increasing liraglutide treatment resulted in dose-dependent reductions in both serum iron and transferrin receptor 1 levels. As shown in Figure 1, the high-dose treatment group (G5) achieved mean values for both serum iron (174.71 ± 23.34 µg/dL) and transferrin receptor 1 (5.16 ± 1.40) that were not significantly different from those of the negative control group (G1), reflecting the effective normalization of iron status.

Oxidative stress markers

The data in Figures 2 and 3 show highly significant differences in both MDA and SOD levels among the study groups. The normal control group (G1) established baseline oxidative stress markers with MDA at 1.55 ± 0.26 nmol/mL and SOD at 73.0 ± 9.2 ng/mL. In contrast, the HFD group (G2) showed significant oxidative stress, evidenced by elevated MDA levels (5.10 ± 0.73 nmol/mL, $P < 0.01$) and increased SOD activity (138.5 ± 23.1 ng/mL, $P < 0.01$), indicating both increased lipid peroxidation and a compensatory antioxidant response.

As shown in Figures 2 and 3, liraglutide treatment demonstrated dose-dependent protective effects against HFD-induced oxidative stress. The lowest dose (100 µg/kg,

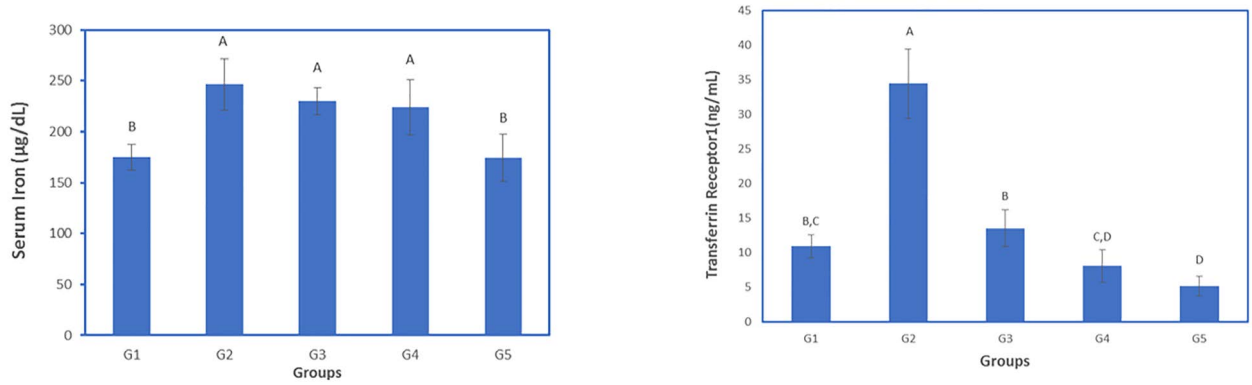

Figure 1. Iron and transferrin receptor-1 levels across different experimental groups. Groups sharing the same letter are not significantly different ($P > 0.05$)

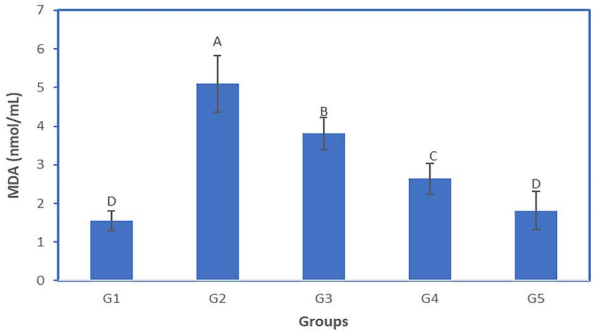

Figure 2. MDA levels across different experimental groups. Groups sharing the same letter are not significantly different ($P > 0.05$)

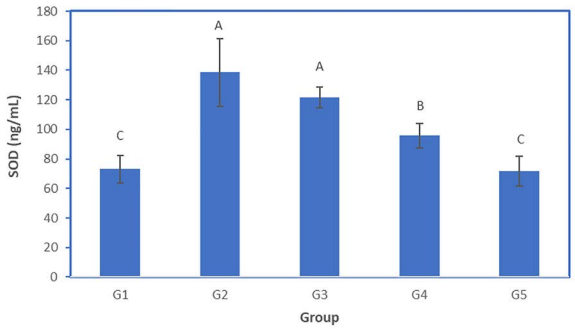

Figure 3. SOD levels across different experimental groups. Groups sharing the same letter are not significantly different ($P > 0.05$)

G3) partially mitigated these changes, reducing MDA to 3.81 ± 0.42 nmol/mL ($P < 0.01$ vs HFD) while maintaining elevated SOD at 121.5 ± 7.0 ng/mL ($P < 0.01$ vs HFD). The intermediate dose (200 µg/kg, G4) showed stronger effects, further lowering MDA to 2.64 ± 0.40 nmol/mL ($P < 0.01$) and normalizing SOD to 95.6 ± 8.1 ng/mL ($P < 0.01$). Most notably, the highest liraglutide dose (400 µg/kg, G5) nearly completely reversed the oxidative stress parameters, bringing MDA down to 1.81 ± 0.50 nmol/mL ($P < 0.01$) and SOD to 71.8 ± 10.1 ng/mL ($P < 0.01$), values comparable to normal controls.

Immunohistochemistry analysis - antioxidant defense proteins

Figure 4 presents the effects of liraglutide treatment on the immunohistochemical expression of two key antioxidant and cytoprotective markers, glutathione peroxidase 4 (GPX4) and HO-1, in HFD-induced obese rats.

As presented in Figure 4, the expression of antioxidant defense proteins GPX4 and HO-1 was quantitatively assessed across experimental groups to evaluate the molecular response to HFD-induced oxidative stress and the effect of GLP-1 receptor agonist treatment, For GPX4, the expression was significantly reduced in the HFD group (G2: 0.1224 ± 0.0014) compared to the negative control group (G1: 0.1845 ± 0.0042) indicating impaired antioxidant defense under oxidative stress. Treatment with liraglutide restored GPX4 expression in a dose-dependent manner, with increasing expression from low dose (G3: 0.2312 ± 0.0058), to medium dose (G4: 0.3580 ± 0.0172), and reaching the highest level in the high-dose group (G5: 0.4442 ± 0.0113), which significantly exceeded all other groups.

A similar restorative trend was observed for HO-1. HO-1 was significantly suppressed in the HFD group (G2: 0.0300 ± 0.0024) compared to control (G1: 0.0716 ± 0.0175). Liraglutide treatment led to a dose-dependent increase: G3 (0.1846 ± 0.0098), G4 (0.3834 ± 0.0302), and G5 (0.4378 ± 0.0143), with the high-dose group again showing the highest expression.

The immunohistochemical analysis of liver tissues showed distinct variations in the expression patterns of GPX4 and HO-1 among the experimental groups, as illustrated in Figures 5 and 6, respectively. In the control group (G1), hepatocytes exhibited minimal to weak positive staining, corresponding to Grade 0–1 reactivity. The HFD group (G2) displayed a complete loss or very faint HO-1 and GPX4 immunoreactivity, indicating impaired antioxidant defense. Liraglutide treatment gradually restored both markers in a dose-dependent manner. The low-dose group (G3) demonstrated mild to moderate immunopositivity (Grade 1–2), whereas the medium-dose group (G4) showed moderate to strong staining (Grade 2–3) localized mainly in the cytoplasm of hepatocytes. The high-dose liraglutide group (G5) exhibited intense cytoplasmic immunostaining for

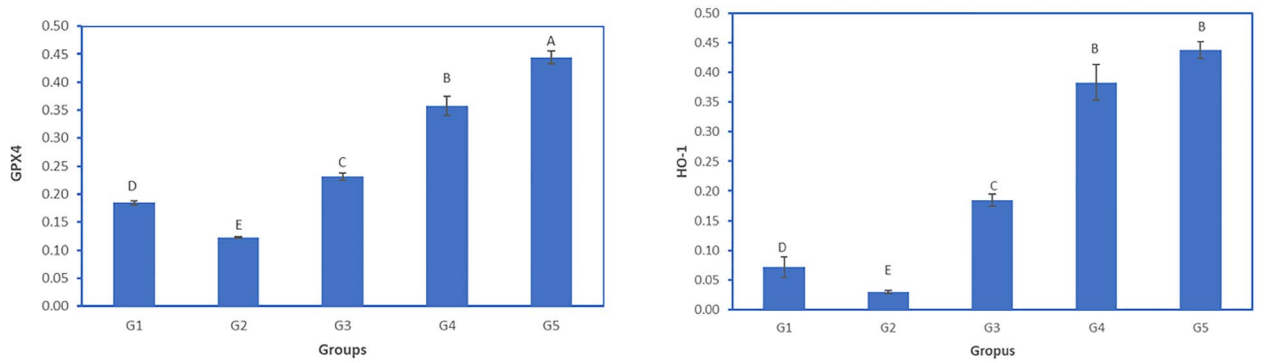

Figure 4. GPX4 And HO-1 expression across different experimental groups. Groups sharing the same letter are not significantly different ($P > 0.05$)

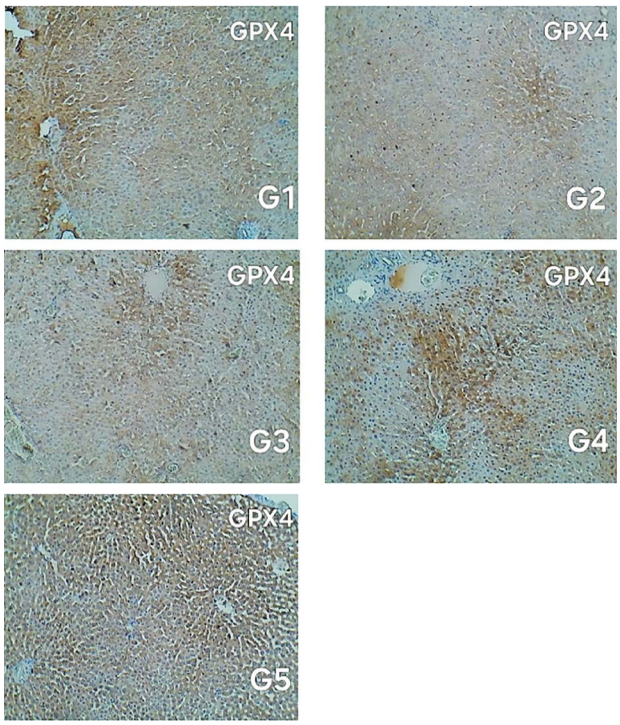

Figure 5. GPX4 immunoexpression of liver tissue (all groups). G1: grade 0 (less than 10%) positive reaction of reactive cells with moderate intensity. G2: grade 0 (less than 10%) reaction of reactive cells with weak intensity. G3: grade 2 (++) positive reaction of reactive cells with severe intensity G4: grade 2 (++) positive reaction of reactive cells with moderate intensity. (100x). G5: grade 3 (+++) positive reaction of reactive cells with severe intensity

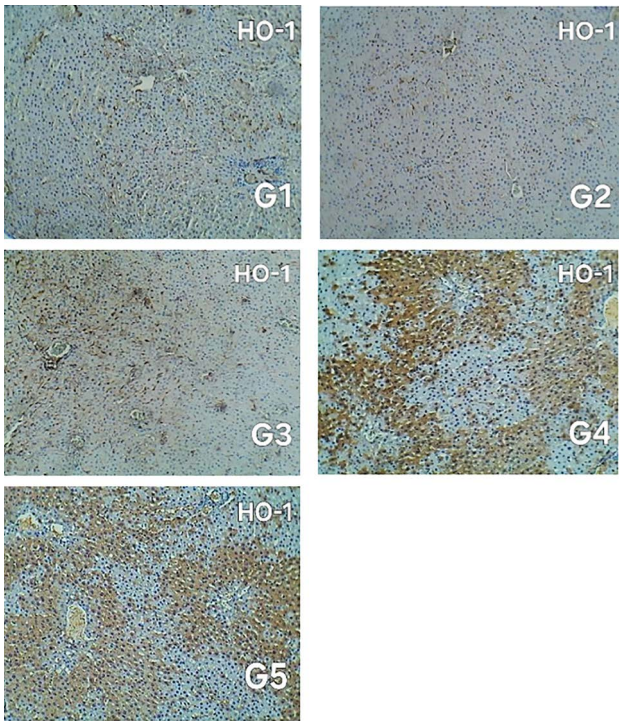

Figure 6. HO-1 immunoexpression of liver tissue. G1: grade 1 (+) positive reaction of reactive cells with very weak intensity. (100x). G2: grade 0, no positive reaction within cells. G3: grade 1(+) positive reaction of reactive cells with weak intensity. (100x). G4: grade 3 (+++) positive reaction of reactive cells with moderate intensity. G5: grade 3 (+++) positive reaction of reactive cells with Severe intensity

both GPX4 and HO-1 (Grade 3), reflecting a marked enhancement of hepatic antioxidant and cytoprotective capacity.

Comparison of HFD and liraglutide on SLC7A11 gene expression

In the assessment of fold change presented in Figure 7, which provides a direct measure of up- or down-regulation in comparison to the control, the high-dose liraglutide group (G5) exhibited the highest mean expression (8.53 ± 4.09), significantly greater than all other groups ($P < 0.05$). Both the medium-dose (G4: 4.25 ± 2.56) and low-dose (G3: 4.11 ± 1.71) groups showed moderate fold increases and were statistically similar to each other (Dunn group B), but significantly higher than the control (G1: 1.51 ± 0.78) and the HFD group (G2: 0.89 ± 0.46). The control (G1) and induction group (G2) represented the lowest levels of fold change and were placed in Dunn groups C and D, respectively, indicating a clear dose-response effect of liraglutide on gene upregulation.

Analysis of the $2^{-\Delta Ct}$ values, which reflect the relative expression of the target gene normalized to the internal control, mirrored the fold change trend. The highest mean expression was observed in G5 (810.80 ± 426.88; Dunn group A), followed by G4 (428.02 ± 281.81) and G3 (375.36 ± 169.60), both grouped in Dunn group B. The control group (G1: 125.12 ± 76.07) and the HFD group (G2: 67.4 ± 43.77) exhibited the lowest normalized

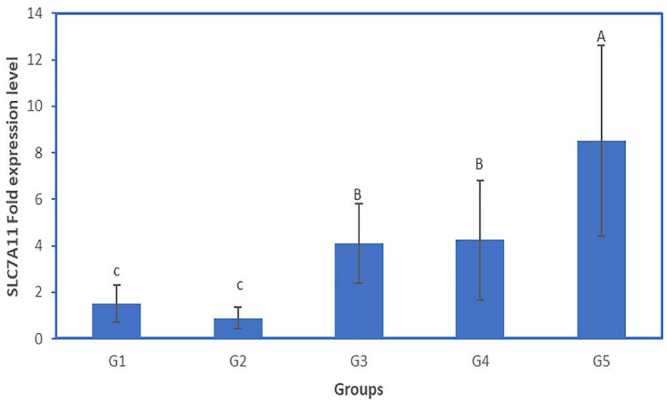

Figure 7. Slc7a11 fold expression level across different experimental groups. Groups sharing the same letter are not significantly different ($P > 0.05$)

expression and were statistically distinct from the treated groups (Dunn groups C and D, respectively).

Discussion

Obesity, particularly when caused by a HFD, is associated with dysregulated iron metabolism, which can lead to oxidative stress and ferroptosis.[22] In this study, the HFD-induced obesity in rats, resulted in a significant increase in serum iron and TfR-1 levels, with G2 group showing the highest values.[23] The therapeutic administration of liraglutide exerted a dose-dependent corrective effect on these parameters, suggesting a restoration of iron homeostasis through liraglutide's multifaceted metabolic actions, including improved insulin sensitivity, reduced inflammation, and attenuation of oxidative stress.[24] Mechanistically, liraglutide may reduce TfR-1 expression through its action on the Nrf2 signaling pathway. Activation of Nrf2 suppressed TfR-1 transcription while promoting the expression of antioxidant proteins such as HO-1 and ferritin, thereby mitigating iron-induced lipid peroxidation and ferroptosis.[25] This finding support the hypothesis that liraglutide's protective effects in obesity extend beyond glycemic control to include modulation of redox-sensitive pathways and iron metabolism. Normalization of iron parameters may also contribute to the suppression of ferroptosis, as iron overload is a critical driver of this cell death modality. By reducing free iron availability, liraglutide helped preserve mitochondrial function and prevent cellular injury in metabolic tissues such as the liver and adipose tissue.[26]

Obesity is also strongly associated with heightened oxidative stress, characterized by an imbalance between pro-oxidants and antioxidant defenses. The current investigation revealed that rats subjected to an HFD (G2) exhibited markedly increased MDA levels, an indicator of lipid peroxidation,[27] and elevated SOD activity, reflecting a compensatory upregulation of antioxidant defenses in response to increased ROS.[28] Liraglutide treatment a significantly reduced these alterations in a dose-dependent manner, demonstrating its capacity to reduce oxidative stress.

HFD-induced obesity leads to systemic oxidative stress via excessive nutrient load, mitochondrial dysfunction, and chronic inflammation.[28] In the liver, this redox imbalance results in lipid peroxidation, cellular damage, and the progression of metabolic diseases.[29] The NRF2 signaling pathway serves as a crucial cellular defense mechanism by regulating the expression of antioxidant genes, including HO-1 and GPX4.[30] Activation of NRF2 protects against oxidative damage and ferroptosis. In this study, HFD-fed rats (G2) exhibited significantly decreased hepatic expression of HO-1 and GPX4 compared with control (G1), indicating compromised antioxidant defenses. These results align with previous findings showing that HFD inhibits NRF2 activity, diminishes antioxidant gene transcription, and increases susceptibility to oxidative liver injury.[31]

The downregulation of GPX4 is particularly noteworthy, as this enzyme is essential for detoxifying lipid peroxides and preventing ferroptosis, hence linking oxidative stress to hepatocellular injury in obesity.[32] Liraglutide treatment counteracted HFD-induced reduction in HO-1 and GPX4 expression in a dose-dependent manner. The high-dose group (G5) exhibited the most pronounced upregulation of HO-1, and GPX4, while medium- (G4) and low-dose (G3) groups showed moderate improvements, indicating partial reactivation of antioxidant pathways. These observations are consistent with previous studies demonstrating that GLP-1 receptor agonists stimulate the NRF2/HO-1 pathway and enhance antioxidant capacity in hepatic and vascular tissues.[33] Liraglutide may act by alleviating endoplasmic reticulum stress, regulating redox-sensitive transcription factors, and improving mitochondrial resilience—mechanisms essential for mitigating obesity-related liver oxidative damage. The HO-1/GPX4 pathway plays a pivotal role in protecting hepatocytes from oxidative damage and ferroptosis, supporting liraglutide's potential as a therapeutic agent in metabolic liver disorders and obesity-related hepatic ferroptosis, including NAFLD/NASH in diabetic or obese individuals.[34]

SLC7A11 encodes the light-chain component of

the cystine/glutamate antiporter (system Xc^-), which facilitates cystine uptake in exchange for glutamate. Cystine is critical for glutathione (GSH) synthesis, establishing SLC7A11 as a key regulator of intracellular redox equilibrium and an inhibitor of ferroptosis through control of iron-dependent lipid peroxidation.[35] Dysregulation of SLC7A11 is implicated in metabolic disorders and oxidative stress-related pathologies, including obesity and insulin resistance.[36] The present investigation, HFD markedly reduced SLC7A11 expression in G2 relative to the control group (G1), as presented in Figure 7 by both fold change and $2^{-\Delta Ct}$ values, consistent with prior linking HFD-induced oxidative stress to suppression of antioxidant defenses in adipose and hepatic tissues, maybe via downregulation of SLC7A11 and GSH synthesis.[37] Reduced SLC7A11 expression suggests a pro-ferroptotic environment in obese states, contributing to metabolic tissue damage and inflammation.

Liraglutide treatment significantly upregulated SLC7A11 expression in a dose-dependent manner, with the high-dose group (G5) exhibiting the highest expression, surpassing all other groups ($P < 0.05$). Medium- and low-dose groups (G4, G3) showed intermediate increases, remaining statistically distinct from control and HFD groups. This restoration and enhancement of SLC7A11 expression likely reflects liraglutide's antioxidant and cytoprotective properties. Previous studies have demonstrated that liraglutide activates Nrf2 signaling pathway, which transcriptionally regulates SLC7A11, HO-1, and other antioxidant genes.[33] The observed gene induction is consistent with liraglutide's broader role in mitigating oxidative damage, preserving mitochondrial integrity, and reducing ferroptosis susceptibility in metabolic tissues.

By upregulation of SLC7A11, liraglutide enhances cystine uptake and GSH synthesis, supporting antioxidant defense and limiting lipid peroxidation. This is especially relevant in obesity, where ferroptosis exacerbates insulin resistance, hepatic steatosis, and adipocyte dysfunction.[31] Thus, the data suggest a novel mechanism by which liraglutide not only corrects metabolic parameters [38] but also restores redox homeostasis at the molecular level.

Conclusion

This study demonstrates that liraglutide significantly modulates key regulators of ferroptosis and antioxidant defense in obesity induced by an HFD. The activation of the HO-1/GPX4 signaling pathway, together with the overexpression of SLC7A11, highlights liraglutide's is pivotal role in enhancing cellular defense mechanisms against oxidative stress and lipid peroxidation in obese rats.

Authors' Contribution

Conceptualization: Mahmood Jameel Saeed, Inam Sameh Arif.
Data curation: Mahmood Jameel Saeed.
Formal analysis: Mahmood Jameel Saeed.
Investigation: Mahmood Jameel Saeed.
Methodology: Mahmood Jameel Saeed, Inam Sameh Arif.
Project administration: Inam Sameh Arif.
Resources: Inam Sameh Arif.
Software: Mahmood Jameel Saeed.
Supervision: Inam Sameh Arif.
Validation: Mahmood Jameel Saeed, Inam Sameh Arif.
Visualization: Mahmood Jameel Saeed.
Writing–original draft: Mahmood Jameel Saeed.
Writing–review & editing: Mahmood Jameel Saeed, Inam Sameh Ari.

Competing Interests

There is no conflict of interest regarding the publication of my manuscript. Funding The research did not receive financial support from an Institution.

Ethical Approval

Ethical approval was obtained from the College of Pharmacy, Mustansiriyah University, Baghdad, Iraq (file no:53, dated 18/10/2024).

Funding

No funding.

References

1. Bray GA, Kim KK, Wilding JP. Obesity: a chronic relapsing progressive disease process. A position statement of the World Obesity Federation. Obes Rev. 2017;18(7):715-23. doi: 10.1111/obr.12551
2. Qasim A, Turcotte M, de Souza RJ, Samaan MC, Champredon D, Dushoff J, et al. On the origin of obesity: identifying the biological, environmental and cultural drivers of genetic risk among human populations. Obes Rev. 2018;19(2):121-49. doi: 10.1111/obr.12625
3. Snezhkina AV, Kudryavtseva AV, Kardymon OL, Savvateeva MV, Melnikova NV, Krasnov GS, et al. ROS generation and antioxidant defense systems in normal and malignant cells. Oxid Med Cell Longev. 2019;2019:6175804. doi: 10.1155/2019/6175804
4. Yang WS, Stockwell BR. Synthetic lethal screening identifies compounds activating iron-dependent, nonapoptotic cell death in oncogenic-RAS-harboring cancer cells. Chem Biol. 2008;15(3):234-45. doi: 10.1016/j.chembiol.2008.02.010
5. Yang WS, Kim KJ, Gaschler MM, Patel M, Shchepinov MS, Stockwell BR. Peroxidation of polyunsaturated fatty acids by lipoxygenases drives ferroptosis. Proc Natl Acad Sci U S A. 2016;113(34):E4966-75. doi: 10.1073/pnas.1603244113
6. Ma W, Jia L, Xiong Q, Du H. Iron overload protects from obesity by ferroptosis. Foods. 2021;10(8):1787. doi: 10.3390/foods10081787
7. Chen YC, Wu YT, Wei YH. Depletion of mitoferrins leads to mitochondrial dysfunction and impairment of adipogenic differentiation in 3T3-L1 preadipocytes. Free Radic Res. 2015;49(11):1285-95. doi: 10.3109/10715762.2015.1067695
8. Moreno-Navarrete JM, Ortega F, Moreno M, Ricart W, Fernández-Real JM. Fine-tuned iron availability is essential to achieve optimal adipocyte differentiation and mitochondrial biogenesis. Diabetologia. 2014;57(9):1957-67. doi: 10.1007/s00125-014-3298-5
9. Zhang Z, Funcke JB, Zi Z, Zhao S, Straub LG, Zhu Y, et al. Adipocyte iron levels impinge on a fat-gut crosstalk to regulate intestinal lipid absorption and mediate protection from obesity. Cell Metab. 2021;33(8):1624-39.e9. doi: 10.1016/j.cmet.2021.06.001
10. Suzuki T, Yamamoto M. Molecular basis of the Keap1-Nrf2 system. Free Radic Biol Med. 2015;88(Pt B):93-100. doi: 10.1016/j.freeradbiomed.2015.06.006

11. Hammadi NA, Al-Mulla Hummadi YM, Waheed HJ. Nebivolol effect on oxidative biomarkers in tamoxifen-induced hepatotoxicity in female white albino rats: in vivo study. Al-Mustansiriyah J Pharm Sci. 2025;25(2):203-11. doi: 10.32947/ajps.v25i2.1157
12. Ryter SW, Alam J, Choi AM. Heme oxygenase-1/carbon monoxide: from basic science to therapeutic applications. Physiol Rev. 2006;86(2):583-650. doi: 10.1152/physrev.00011.2005
13. Croom KF, McCormack PL. Liraglutide: a review of its use in type 2 diabetes mellitus. Drugs. 2009;69(14):1985-2004. doi: 10.2165/11201060-000000000-00000
14. Astrup A, Carraro R, Finer N, Harper A, Kunesova M, Lean ME, et al. Safety, tolerability and sustained weight loss over 2 years with the once-daily human GLP-1 analog, liraglutide. Int J Obes (Lond). 2012;36(6):843-54. doi: 10.1038/ijo.2011.158
15. Alshehri GH, Al-Kuraishy HM, Waheed HJ, Al-Gareeb AI, Faheem SA, Alexiou A, et al. Tirzepatide: a novel therapeutic approach for Alzheimer's disease. Metab Brain Dis. 2025;40(5):221. doi: 10.1007/s11011-025-01649-z
16. Lu C, Xu C, Li S, Ni H, Yang J. Liraglutide and GLP-1(9-37) alleviated hepatic ischemia-reperfusion injury by inhibiting ferroptosis via GSK3β/Nrf2 pathway and SMAD159/Hepcidin/FTH pathway. Redox Biol. 2025;79:103468. doi: 10.1016/j.redox.2024.103468
17. Chen X, Wang T, Gao Y, Wang GA, Guan J, Dai H. Liraglutide suppresses ferroptosis by upregulation Nrf2 in type 2 diabetic cardiomyopathy. Peptides. 2025;192:171429. doi: 10.1016/j.peptides.2025.171429
18. Palleria C, Leo A, Andreozzi F, Citraro R, Iannone M, Spiga R, et al. Liraglutide prevents cognitive decline in a rat model of streptozotocin-induced diabetes independently from its peripheral metabolic effects. Behav Brain Res. 2017;321:157-69. doi: 10.1016/j.bbr.2017.01.004
19. Zandieh S, Hopf R, Redl H, Schlag MG. The effect of ketamine/xylazine anesthesia on sensory and motor evoked potentials in the rat. Spinal Cord. 2003;41(1):16-22. doi: 10.1038/sj.sc.3101400
20. Parasuraman S, Raveendran R, Kesavan R. Blood sample collection in small laboratory animals. J Pharmacol Pharmacother. 2010;1(2):87-93. doi: 10.4103/0976-500x.72350
21. Smith GL, Reutovich AA, Srivastava AK, Reichard RE, Welsh CH, Melman A, et al. Complexation of ferrous ions by ferrozine, 2,2′-bipyridine and 1,10-phenanthroline: implication for the quantification of iron in biological systems. J Inorg Biochem. 2021;220:111460. doi: 10.1016/j.jinorgbio.2021.111460
22. Stockwell BR, Friedmann Angeli JP, Bayir H, Bush AI, Conrad M, Dixon SJ, et al. Ferroptosis: a regulated cell death nexus linking metabolism, redox biology, and disease. Cell. 2017;171(2):273-85. doi: 10.1016/j.cell.2017.09.021
23. Ganz T, Nemeth E. Iron metabolism: interactions with normal and disordered erythropoiesis. Cold Spring Harb Perspect Med. 2012;2(5):a011668. doi: 10.1101/cshperspect.a011668
24. Drucker DJ. Mechanisms of action and therapeutic application of glucagon-like peptide-1. Cell Metab. 2018;27(4):740-56. doi: 10.1016/j.cmet.2018.03.001
25. Kerins MJ, Ooi A. The roles of Nrf2 in modulating cellular iron homeostasis. Antioxid Redox Signal. 2018;29(17):1756-73. doi: 10.1089/ars.2017.7176
26. Latunde-Dada GO. Ferroptosis: Role of lipid peroxidation, iron and ferritinophagy. Biochim Biophys Acta Gen Subj. 2017;1861(8):1893-900. doi: 10.1016/j.bbagen.2017.05.019
27. Khalif AA, Mshimesh BA, Abood DA, Al-Qaysi SA. Comparative analysis of inflammatory and oxidative stress indicators in rat models of CKD induced by adenine versus folic acid; an experimental study. J Nephropathol. 2025;14(3):e27617. doi: 10.34172/jnp.2025.27617
28. Furukawa S, Fujita T, Shimabukuro M, Iwaki M, Yamada Y, Nakajima Y, et al. Increased oxidative stress in obesity and its impact on metabolic syndrome. J Clin Invest. 2004;114(12):1752-61. doi: 10.1172/jci21625
29. Poli G, Albano E, Dianzani MU. The role of lipid peroxidation in liver damage. Chem Phys Lipids. 1987;45(2-4):117-42. doi: 10.1016/0009-3084(87)90063-6
30. Arif IS, Raoof IB, Luaibi HH. Nuclear factor erythroid-2 linked factor (Nrf2) as a potential mediator of hepatotoxicity. Al-Mustansiriyah J Pharm Sci. 2021;21(4):12-6. doi: 10.32947/ajps.v21i4.796
31. Bozadjieva-Kramer N, Shin JH, Blok NB, Jain C, Das NK, Polex-Wolf J, et al. Liraglutide impacts iron homeostasis in a murine model of hereditary hemochromatosis. Endocrinology. 2024;165(9):bqae090. doi: 10.1210/endocr/bqae090
32. Jiang X, Stockwell BR, Conrad M. Ferroptosis: mechanisms, biology and role in disease. Nat Rev Mol Cell Biol. 2021;22(4):266-82. doi: 10.1038/s41580-020-00324-8
33. Lin T, Zhang Y, Wei Q, Huang Z. GLP-1 receptor agonist liraglutide alleviates kidney injury by regulating nuclear translocation of Nrf2 in diabetic nephropathy. Clin Exp Pharmacol Physiol. 2024;51(12):e70003. doi: 10.1111/1440-1681.70003
34. Nevola R, Epifani R, Imbriani S, Tortorella G, Aprea C, Galiero R, et al. GLP-1 receptor agonists in non-alcoholic fatty liver disease: current evidence and future perspectives. Int J Mol Sci. 2023;24(2):1703. doi: 10.3390/ijms24021703
35. Dixon SJ, Lemberg KM, Lamprecht MR, Skouta R, Zaitsev EM, Gleason CE, et al. Ferroptosis: an iron-dependent form of nonapoptotic cell death. Cell. 2012;149(5):1060-72. doi: 10.1016/j.cell.2012.03.042
36. Lin W, Wang C, Liu G, Bi C, Wang X, Zhou Q, et al. SLC7A11/xCT in cancer: biological functions and therapeutic implications. Am J Cancer Res. 2020;10(10):3106-26.
37. Yang WS, Stockwell BR. Ferroptosis: death by lipid peroxidation. Trends Cell Biol. 2016;26(3):165-76. doi: 10.1016/j.tcb.2015.10.014
38. Rizzo M, Rizvi AA, Patti AM, Nikolic D, Giglio RV, Castellino G, et al. Liraglutide improves metabolic parameters and carotid intima-media thickness in diabetic patients with the metabolic syndrome: an 18-month prospective study. Cardiovasc Diabetol. 2016;15(1):162. doi: 10.1186/s12933-016-0480-8